Int. J. Appl. Comput. Math (2023) 9:43
https://doi.org/10.1007/s40819-023-01523-5

ORIGINAL PAPER

New Fractional Modelling and Simulations of Prey–Predator System with Mittag–Leffler Kernel

Mohammad Partohaghighi[1] · Ali Akgül[2,3]

Accepted: 14 April 2023 / Published online: 11 May 2023

Abstract
Predator–prey models are regarded as the structural blocks of the bio- and ecosystems as biomasses are headed by their resource masses. During the current investigation, we examine the impact of a contagious disease on the growth of ecological varieties. We study a non-integer-order predator–prey system by applying the Atangana–Baleanu–Caputo derivative. We use an effective techniqueto get the numerical solutions and to discover the system's dynamical behavior using different values of fractional order which indicates that how how the proposed scheme is suitable to solve the dynamical systems containing the derivatives with non-singular kernels. Moreover, the existence of the results is given utilizing the fixed-point theorem. Also, diagrams via numerical simulations of the approximate solutions are shown in different dimensions.

Keywords Mittag–Leffler kernel · Atangana–Baleanu derivative · Non-singular kernel · Predator–prey system · Fixed point analysis

Introduction

The evolution of the qualitative investigation of ODEs is arising to analyze various enigmas in mathematical biology and related areas. Designing the model to the community dynamics of a prey–predator problem is an example of the significant and impressive aim in mathematical biology, that has undergone comprehensive reflection by many scholars [1–6]. During real universe, several classes of prey and predator classes possess a living past which is formed of at least couple steps: immature and mature, and every step possesses various behavioral characteristics. Therefore, some activities of step-building prey–predator systems are presented in many articles in the literature [7–12]. Contagious diseases occur if infected external bodies penetrate into the individual body.

✉ Ali Akgül
aliakgul00727@gmail.com

1 Department of Mathematics, Clarkson University, Potsdam, NY 13699, USA

2 Art and Science Faculty, Department of Mathematics, Siirt University, 56100 Siirt, Turkey

3 Department of Electronics and Communication Engineering, Saveetha School of Engineering, SIMATS, Chennai, Tamilnadu, India

Table 1 Vital parameters involved in the eco-epidemiological system

Parameters	Description
ξ_1	Reproduction number of the prey population
$(\xi_2 + \xi_3 u_3(t))u_3(t)u_1(t)$	
$\&(\xi_2 + \xi_3 u_3(t))u_3(t)u_2(t)$	Hunting cooperation functional
ξ_4	Transmission rate of the prey population (infection rate)
ξ_5	Death rate of the prey population
ξ_6	Conversion rate of prey biomass into predator biomass
ξ_7	Natural mortality of the predator population

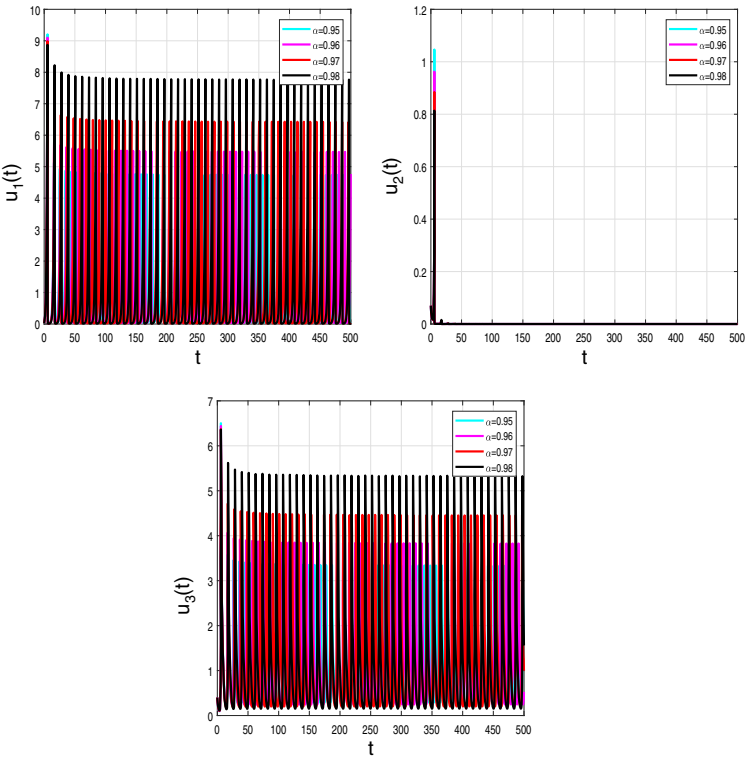

Fig. 1 Numerical simulations for $u_1(0) = 0.01$, $u_2(0) = 1.1$ and $u_3(0) = 0.05$ for $\xi_1 = 1.5$, $\xi_2 = 1.5$, $\xi_3 = 0.5$, $\xi_4 = 0.5$, $\xi_5 = 0.5$, $\xi_6 = 0.5$ and $\xi_7 = 0.5$

The mentioned pathogens could be bacteria, microorganisms, and parasites. These bodies are transferred by virus from a different individual, creatures, polluted food, or disposal to any of the environmental constituents which are infected by any of the mentioned organisms. These diseases have several signs in body, containing raised one warmth and anxiety, moreover to additional traits which vary regarding the position of contamination, nature, and hardness of the infection. It is permissible to possess a disease that produces moderate signs, and hence it does not require to be solved. Indeed, there are severe situations that may affect mortality. Also, they probably influence the population scale of several kinds. In a

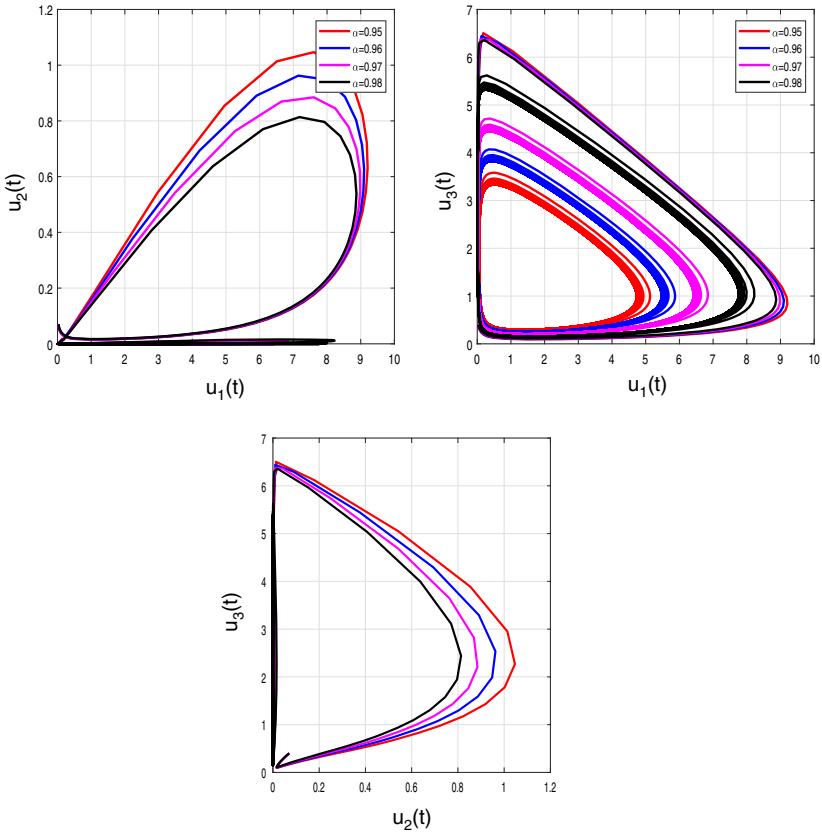

Fig. 2 Numerical simulations for $u_1(0) = 0.01$, $u_2(0) = 1.1$ and $u_3(0) = 0.05$ for $\xi_1 = 1.5$, $\xi_2 = 1.5$, $\xi_3 = 0.5$, $\xi_4 = 0.5$, $\xi_5 = 0.5$, $\xi_6 = 0.5$ and $\xi_7 = 0.5$

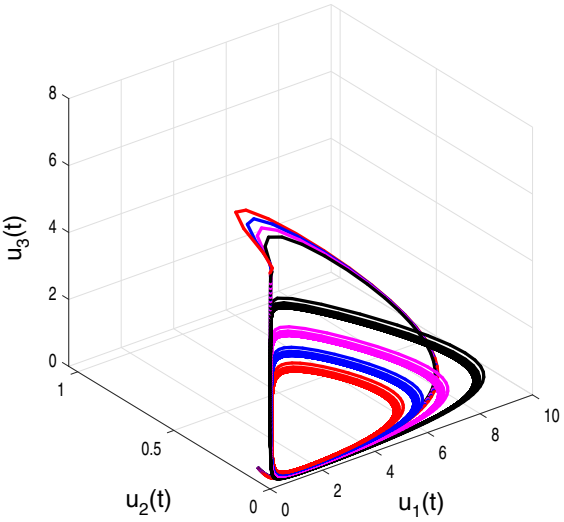

Fig. 3 Chaotic behaviour of solutions for $u_1(0) = 0.01$, $u_2(0) = 1.1$ and $u_3(0) = 0.05$ for $\xi_1 = 1.5$, $\xi_2 = 1.5$, $\xi_3 = 0.5$, $\xi_4 = 0.5$, $\xi_5 = 0.5$, $\xi_6 = 0.5$ and $\xi_7 = 0.5$

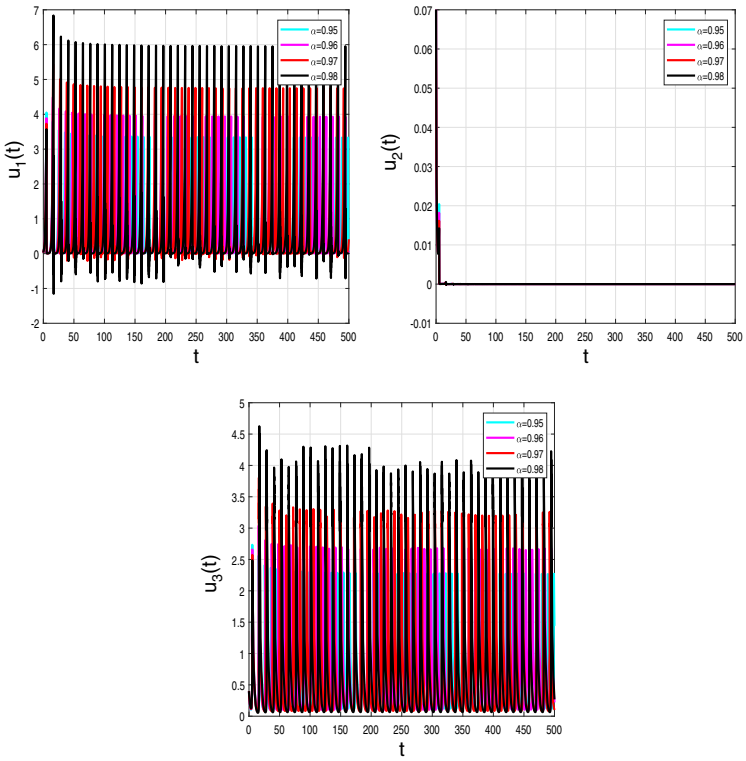

Fig. 4 Numerical simulations for $u_1(0) = 0.01$, $u_2(0) = 1.1$ and $u_3(0) = 0.05$ for $\xi_1 = 1.5$, $\xi_2 = 0.5$, $\xi_3 = 0.5$, $\xi_4 = 0.5$, $\xi_5 = 0.5$, $\xi_6 = 0.5$ and $\xi_7 = 0.5$

more dangerous situation, some species probably indeed become dead because of some fatal infections that occurred in some extremely rational populations. Mathematical systems for foretelling the progression of varieties of such pathogen have been utilized in an escalating way in the latest decades. The biological species are most susceptible to any disease that can affect the development of species. We study the predator–prey interplay. Such disease is able to influence the power of predators and performance of shooting, which places some predators at threat of extirpation. During the literature review, several investigations were examined on the predator–prey interplay in bearing the contagious infections [12–16].

On the other hand, there are various approaches that the predators examine for reaching prosperous hunting. Predator assistance is an efficient approach that several predators seek a unique prey. Such an approach can be so beneficial in degrading the hunting failure scale. Numerous anglers perform in the aforementioned approach. For instance, some animals such as lions, and dogs are distinguished for the great ability scale in this manner. Numerical solution of two- sided space-fractional wave equation using finite difference method in [17]. Modelling of such particular performance of predator was firstly formed in [18]. wherein an uncomplicated pattern was employed for representing such collaboration. There were studies that investigated such performance in the predator–prey interplay [19–27]. Regarding the achieved outcomes in [28], time-fractional derivative possesses wide applicability for explaining various real-life conditions, that is recognized with memory impact for the dynamical model; memory speed is named for non-integer order, memory function of kernel

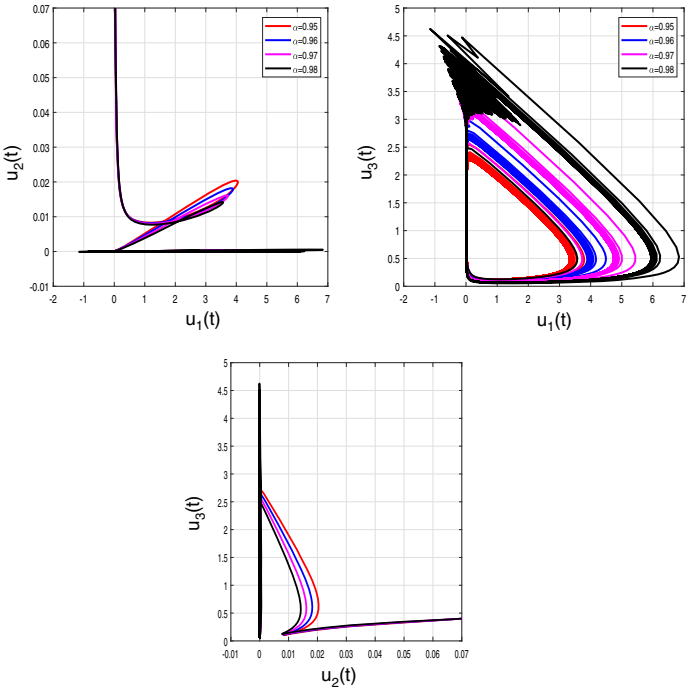

Fig. 5 Numerical simulations for $u_1(0) = 0.01$, $u_2(0) = 1.1$ and $u_3(0) = 0.05$ for $\xi_1 = 1.5$, $\xi_2 = 0.5$, $\xi_3 = 0.5$, $\xi_4 = 0.5$, $\xi_5 = 0.5$, $\xi_6 = 0.5$ and $\xi_7 = 0.5$

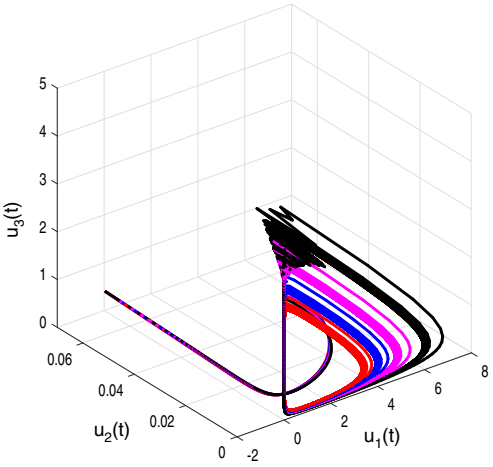

Fig. 6 Chaotic behaviour of solutions for $u_1(0) = 0.01$, $u_2(0) = 1.1$ and $u_3(0) = 0.05$ for $\xi_1 = 1.5$, $\xi_2 = 0.5$, $\xi_3 = 0.5$, $\xi_4 = 0.5$, $\xi_5 = 0.5$, $\xi_6 = 0.5$ and $\xi_7 = 0.5$

of non-integer derivative. The mentioned derivative Atangana–Baleanu–Caputo (ABC) is applied to model several phenomena [29–32]. More studies about the applications of fractional operators can be found in [33–37]. Regarding the mentioned inclinations, we examine the eco-epidemiological system given below:

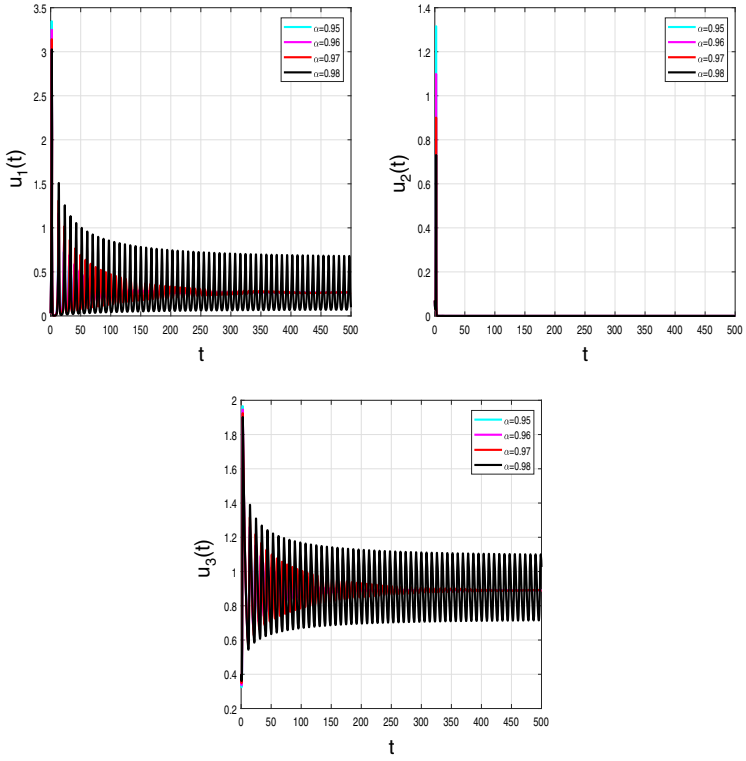

Fig. 7 Numerical simulations for $u_1(0) = 0.01$, $u_2(0) = 1.1$ and $u_3(0) = 0.05$ for $\xi_1 = 3.5$, $\xi_2 = 3.05$, $\xi_3 = 0.8$, $\xi_4 = 2.5$, $\xi_5 = 0.15$, $\xi_6 = 0.5$ and $\xi_7 = 0.3$

$$\begin{aligned}
\frac{du_1}{dt} &= f_1(u_1, u_2, u_3) = \xi_1(u_1(t) + u_2(t)) - (\xi_2 + \xi_3 u_3(t))u_3(t)u_1(t) \\
&\quad - \xi_4 u_1(t)u_2(t) - \xi_5 u_1(t), \\
\frac{du_2}{dt} &= f_2(u_1, u_2, u_3) = \xi_4 u_1(t)u_2(t) - (\xi_2 + \xi_3 u_3(t))u_3(t)u_2(t) - \xi_5 u_2(t), \\
\frac{du_3}{dt} &= f_3(u_1, u_2, u_3) = \xi_6(\xi_2 + \xi_3 u_3(t))u_3(t)(u_1(t) + u_2(t)) - \xi_7 u_3(t),
\end{aligned} \tag{1}$$

where it may be noted that the state variables $u_1(t)$, $u_2(t)$, and $u_3(t)$ respectively stand for densities of susceptible prey, infected prey, and the predator populations. Regarding initial conditions (ICs), we have $u_1(0) = u_{1,0}(t)$, $u_2(0) = u_{2,0}(t)$ and $u_3(0) = u_{3,0}(t)$. Moreover, one can see that there are 7 parameters playing the vital role for the dynamics of the model's behavior. Description of these parameters is detailed in the Table 1.

The next section is selected to implement some fundamental definitions to comprehend remaining analysis carried out in other forthcoming sections.

Essential Definitions

Definition 2.1 Assume that $X \in H^1(a, b)$, $a < b$ and $\sigma \in [0, 1]$. Therefore, the Atangana-Baleanu derivative for X in the Caputo structure is written as

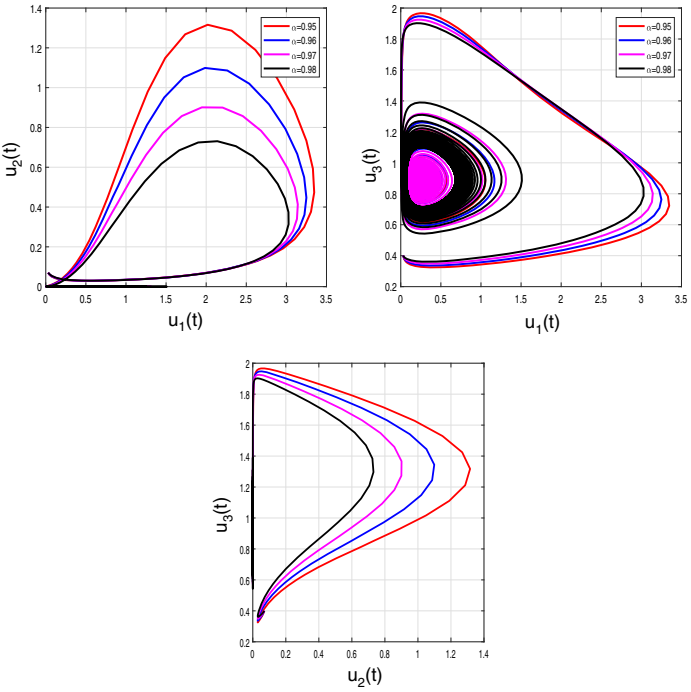

Fig. 8 Numerical simulations for $u_1(0) = 0.01$, $u_2(0) = 1.1$ and $u_3(0) = 0.05$ for $\xi_1 = 3.5$, $\xi_2 = 3.05$, $\xi_3 = 0.8$, $\xi_4 = 2.5$, $\xi_5 = 0.15$, $\xi_6 = 0.5$ and $\xi_7 = 0.3$

Fig. 9 Chaotic behaviour of solutions for $u_1(0) = 0.01$, $u_2(0) = 1.1$ and $u_3(0) = 0.05$ for $\xi_1 = 3.5$, $\xi_2 = 3.05$, $\xi_3 = 0.8$, $\xi_4 = 2.5$, $\xi_5 = 0.15$, $\xi_6 = 0.5$ and $\xi_7 = 0.3$

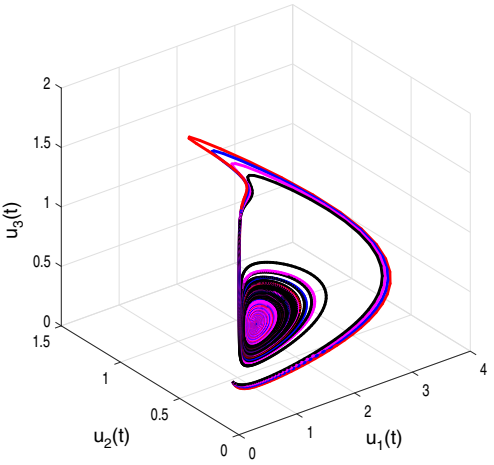

$$ {}^{ABC}\mathcal{D}^{\sigma} X(t) = \frac{W(\sigma)}{1-\sigma} \int_a^t X'(y) E_{\sigma}\left[-\sigma \frac{(t-\zeta)^{\sigma}}{1-\sigma}\right] \mathrm{d}\zeta, \tag{2} $$

where E_σ is known as the Mittag–Leffler function explained in [33, 34].

$$ E_{\sigma}(z) = \sum_{n=0}^{\infty} \frac{z^n}{\Gamma(n\sigma + 1)}, $$

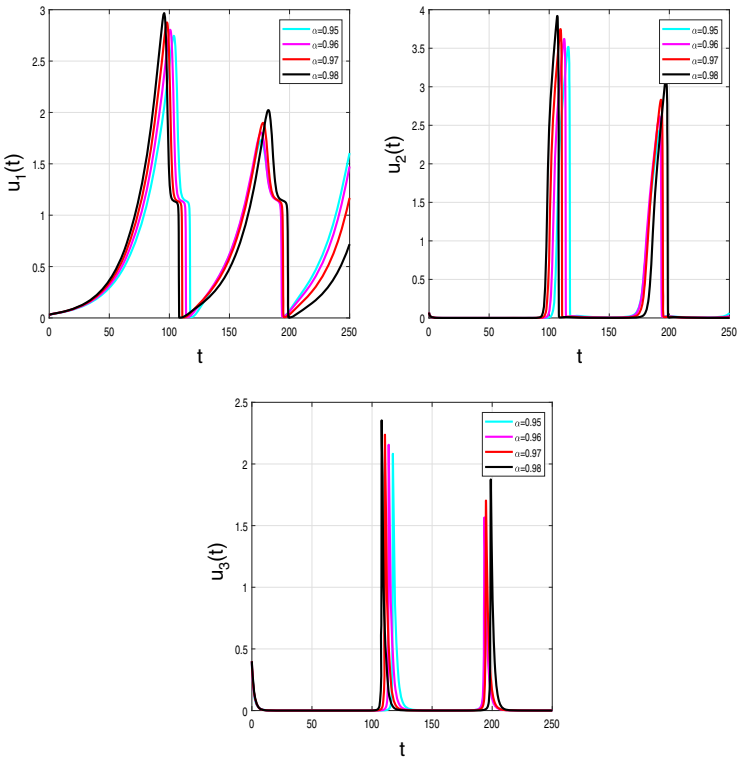

Fig. 10 Numerical simulations for $u_1(0) = 0.01, u_2(0) = 1.1$ and $u_3(0) = 0.05$ for $\xi_1 = 0.55, \xi_2 = 0.5, \xi_3 = 3.5, \xi_4 = 0.5, \xi_5 = 0.5, \xi_6 = 0.5$ and $\xi_7 = 1.5$

Theorem 2.2 *We take into consideration the differential equation containing the Atangana-Baleanu differential operator* [35]*:*

$$^{ABC}{}_0\mathcal{D}_t^{\sigma} f(t) = u(t). \tag{3}$$

The foregoing equation possesses a unique answer if the subsequent theorem is performed

$$f(t) = \frac{1-\sigma}{W(\sigma)}u(t) + \frac{\sigma}{W(\sigma)\Gamma(p)}\int_0^t u(\zeta)(t-\zeta)^{\sigma-1}\mathrm{d}\zeta,$$

The common time-fractional order of the differential equation described in (7) is a problem of the form

$$\mathcal{D}^{\sigma} X(t) = F(X(t), t), \sigma \in (0, 1), \tag{4}$$

Analysis by Non-integer Order

We suppose that $\mathfrak{B} = \mathcal{B}(L) \times \mathcal{B}(L)$, which $\mathcal{B}(L)$ named continuous Branch function on interval L containing

$$\|u_1, u_2, u_3\| = \|u_1\| + \|u_2\| + \|u_3\|\|,$$

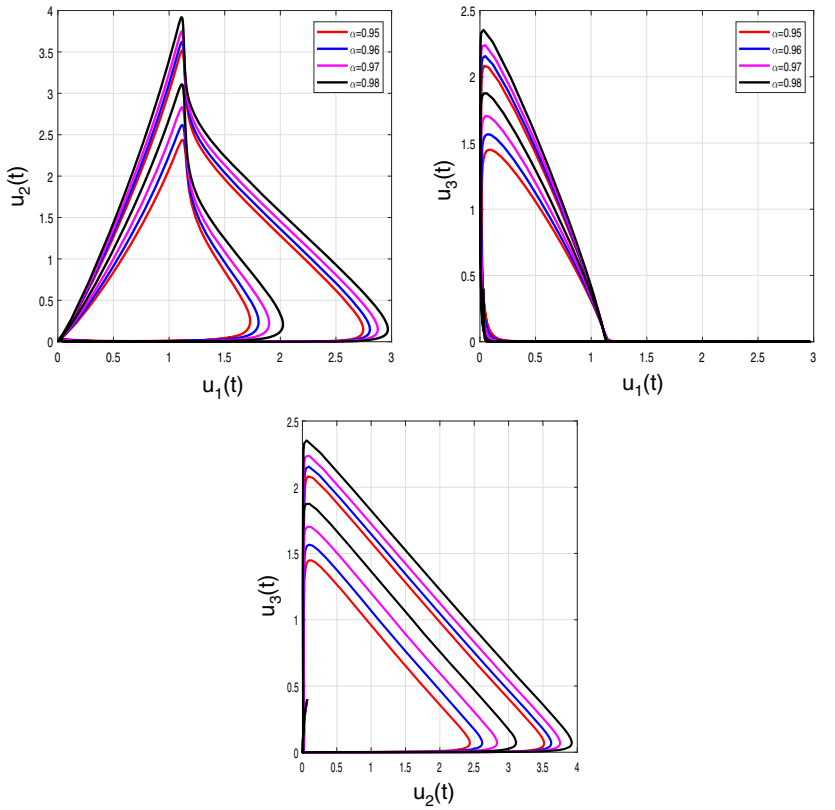

Fig. 11 Numerical simulations for $u_1(0) = 0.01, u_2(0) = 1.1$ and $u_3(0) = 0.05$ for $\xi_1 = 0.55, \xi_2 = 0.5, \xi_3 = 3.5, \xi_4 = 0.5, \xi_5 = 0.5, \xi_6 = 0.5$ and $\xi_7 = 1.5$

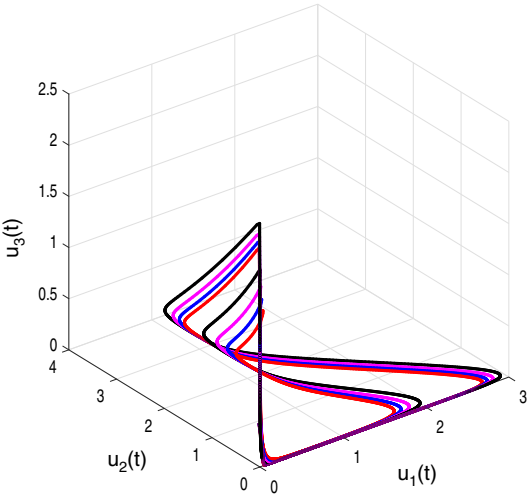

Fig. 12 Chaotic behaviour of solutions for $u_1(0) = 0.01, u_2(0) = 1.1$ and $u_3(0) = 0.05$ for $\xi_1 = 0.55, \xi_2 = 0.5, \xi_3 = 3.5, \xi_4 = 0.5, \xi_5 = 0.5, \xi_6 = 0.5$ and $\xi_7 = 1.5$

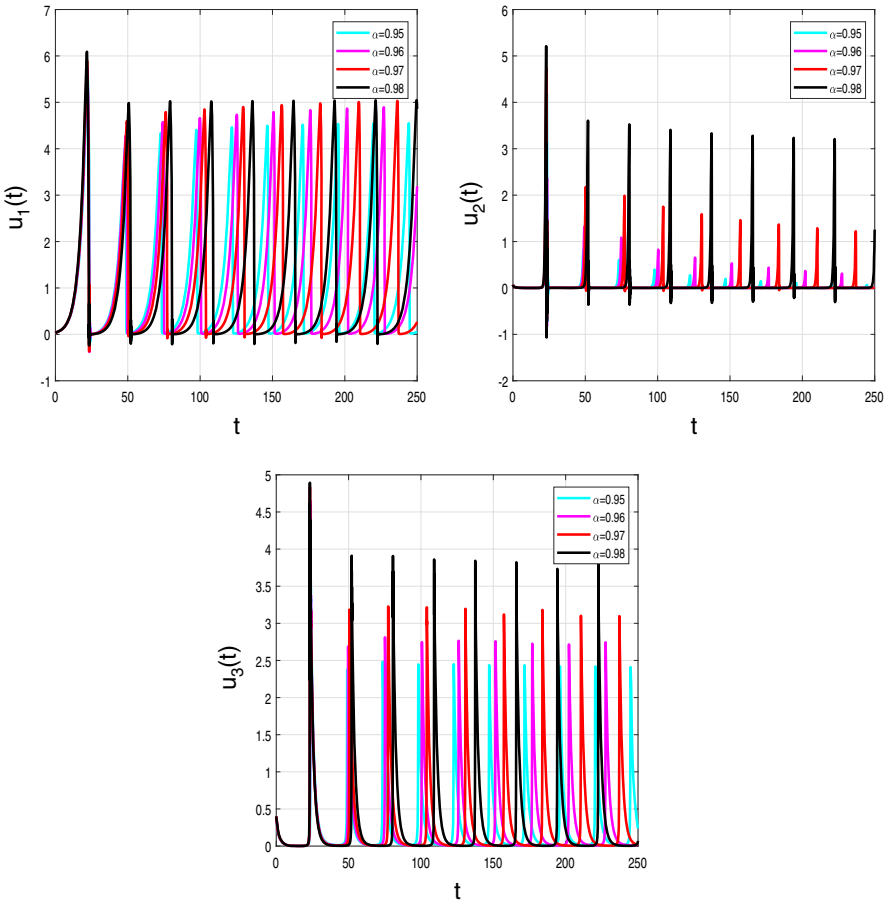

Fig. 13 Numerical simulations for $u_1(0) = 0.01, u_2(0) = 1.1$ and $u_3(0) = 0.05$ for $\xi_1 = 0.75, \xi_2 = 0.5, \xi_3 = 3.5, \xi_4 = 0.5, \xi_5 = 0.5, \xi_6 = 0.5$ and $\xi_7 = 1.5$

which $\|u_1\| = \sup\{|u_1(t) : t \in L\}$, $\|u_2\| = \sup\{|u_2(t) : t \in L\}$ and $\|u_3\| = \sup\{|u_3(t) : t \in L\}$, Following, we develop the problem (1) by interchanging the traditional derivative by ABC one:

$$\begin{aligned}
{}^{ABC}{}_0\mathcal{D}_t^{\sigma} u_1(t) &= \xi_1(u_1(t) + u_2(t)) - (\xi_2 + \xi_3 u_3)u_3(t)u_1(t) - \xi_4 u_1(t)u_2(t) - \xi_5 u_1(t),\\
{}^{ABC}{}_0\mathcal{D}_t^{\sigma} u_2(t) &= \xi_4 u_1(t)u_2(t) - (\xi_2 + \xi_3 u_3)u_3(t)u_2(t),\\
{}^{ABC}{}_0\mathcal{D}_t^{\sigma} u_3(t) &= \xi_5(\xi_2 + \xi_3 u_3(t))u_3(t)(u_1(t) + u_2(t)) - \xi_5,
\end{aligned} \tag{5}$$

Regarding ICs

$$u_1(0) = u_{1,0}(t), u_2(0) = u_{2,0}(t), u_3(0) = u_{3,0}(t), \tag{6}$$

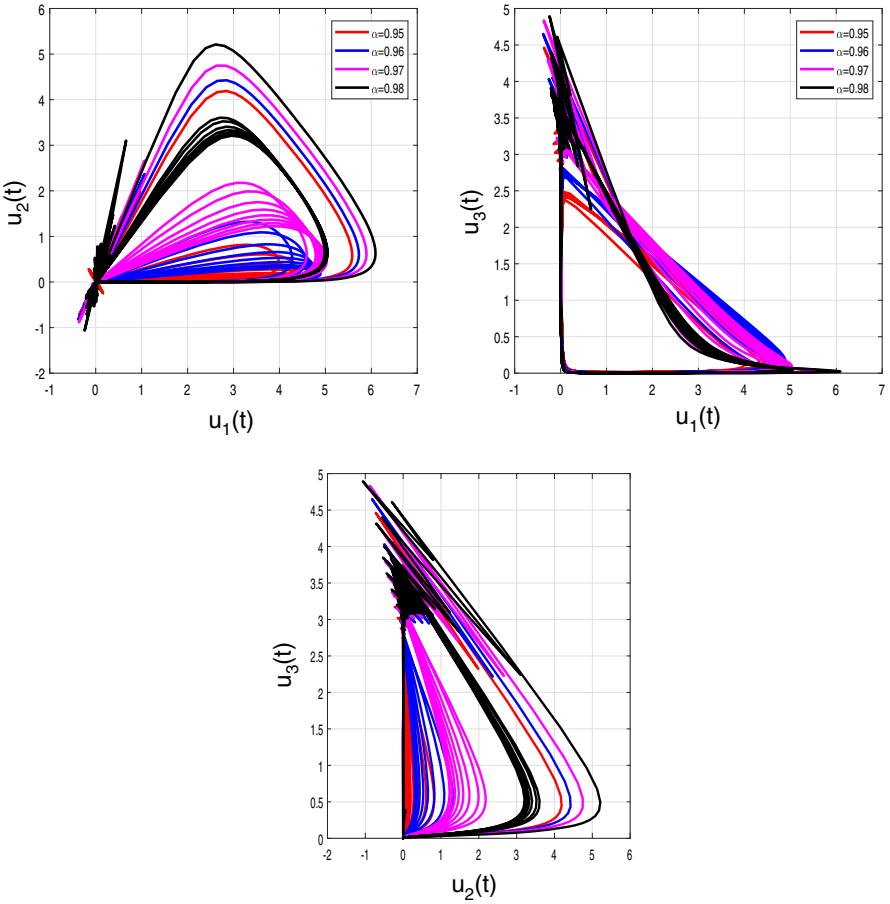

Fig. 14 Numerical simulations for $u_1(0) = 0.01, u_2(0) = 1.1$ and $u_3(0) = 0.05$ for $\xi_1 = 0.75, \xi_2 = 0.5, \xi_3 = 3.5, \xi_4 = 0.5, \xi_5 = 0.5, \xi_6 = 0.5$ and $\xi_7 = 1.5$

We have

$$
\begin{aligned}
u_1(t) - u_1(0) &= \frac{1-\sigma}{W(\sigma)}\left[\xi_1(u_1(t)+u_2(t)) - (\xi_2+\xi_3u_3)u_3(t)u_1(t) - \xi_4u_1(t)u_2(t) - \xi_5u_1(t)\right] \\
&\quad + \frac{\sigma}{W(\sigma)\Gamma(\sigma)}\int_0^t (t-\zeta)^{\sigma-1} \times \left[\xi_1(u_1(t)+u_2(t)) - (\xi_2+\xi_3u_3)u_3(t)u_1(t)\right. \\
&\quad \left. -\xi_4u_1(t)u_2(t) - \xi_5u_1(t)\right]\mathrm{d}\zeta, \\
u_2(t) - u_2(0) &= \frac{1-\sigma}{W(\sigma)}\left[\xi_4u_1(t)u_2(t) - (\xi_2+\xi_3u_3)u_3(t)u_2(t)\right] \\
&\quad + \frac{\sigma}{W(\sigma)\Gamma(\sigma)}\int_0^t (t-\zeta)^{\sigma-1} \times \left[\xi_4u_1(t)u_2(t) - (\xi_2+\xi_3u_3)u_3(t)u_2(t)\right]\mathrm{d}\zeta, \\
u_3(t) - u_3(0) &= \frac{1-\sigma}{W(\sigma)}\left[\xi_5(\xi_2+\xi_3u_3(t))u_3(t)(u_1(t)+u_2(t)) - \xi_5\right] \\
&\quad + \frac{\sigma}{W(\sigma)\Gamma(\sigma)}\int_0^t (t-\zeta)^{\sigma-1} \times \left[\xi_6(\xi_2+\xi_3u_3(t))u_3(t)(u_1(t)+u_2(t)) - \xi_7u_3(t)\right]\mathrm{d}\zeta, \quad (7)
\end{aligned}
$$

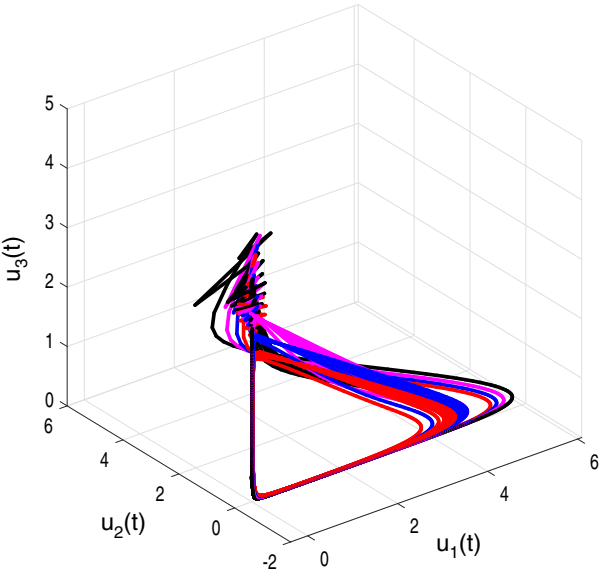

Fig. 15 Chaotic behaviour of solutions for $u_1(0) = 0.01, u_2(0) = 1.1$ and $u_3(0) = 0.05$ for $\xi_1 = 0.75, \xi_2 = 0.5, \xi_3 = 3.5, \xi_4 = 0.5, \xi_5 = 0.5, \xi_6 = 0.5$ and $\xi_7 = 1.5$

Now, we take

$$\begin{aligned}
\mathcal{B}_1(u_1, t) &= \xi_1(u_1(t) + u_2(t)) - (\xi_2 + \xi_3 u_3)u_3(t)u_1(t) - \xi_4 u_1(t)u_2(t) - \xi_5 u_1(t) \\
\mathcal{B}_2(u_2, t) &= [\xi_4 u_1(t)u_2(t) - (\xi_2 + \xi_3 u_3)u_3(t)u_2(t) \\
\mathcal{B}_3(u_3, t) &= \xi_6(\xi_2 + \xi_3 u_3(t))u_3(t)(u_1(t) + u_2(t)) - \xi_7 u_3(t)
\end{aligned} \tag{8}$$

Beside, we provide the subsequent result.

Lemma 3.1 *The kernels* $\mathcal{B}_i(u_i, t)$, *for* $i = 1, 2, 3$ *hold the Lipschitz condition for* $0 \leq \mathcal{B}_i(u_i, t) < 1, i = 1, 2, 3$.

Proof Opening by $i = 2$ we own $\mathcal{B}_2(u_1, t) = \xi_4 u_1(t)u_2(t) - (\xi_2 + \xi_3 u_3)u_3(t)u_2(t)$. Let u_1 and u_1^*, the we own

$$\begin{aligned}
\|\mathcal{B}_2(u_1, t) - \mathcal{B}_2(u_1^*, t)\| &= \| - \xi_4 \left\{u_2(t) - u_2^*(t)\right\} \| \\
&\leq \|\xi_4\| \|u_2(t) - u_2^*(t)\| \leq G_2 \|u_2(t) - u_2^*(t)\|
\end{aligned} \tag{9}$$

which $G_2 = \xi_4$. Take $m_1 = \max_{t \in L} \|u_1(t)\|$, $m_2 = \max_{t \in L} \|u_2(t)\|$ and $m_3 = \max_{t \in L} \|u_3(t)\|$ be limited functions, so

$$\|\mathcal{B}_1(u_2, t) - \mathcal{B}_1(u_2^*, t)\| \leq G_2 \|u_2(t) - u_2^*(t)\|$$

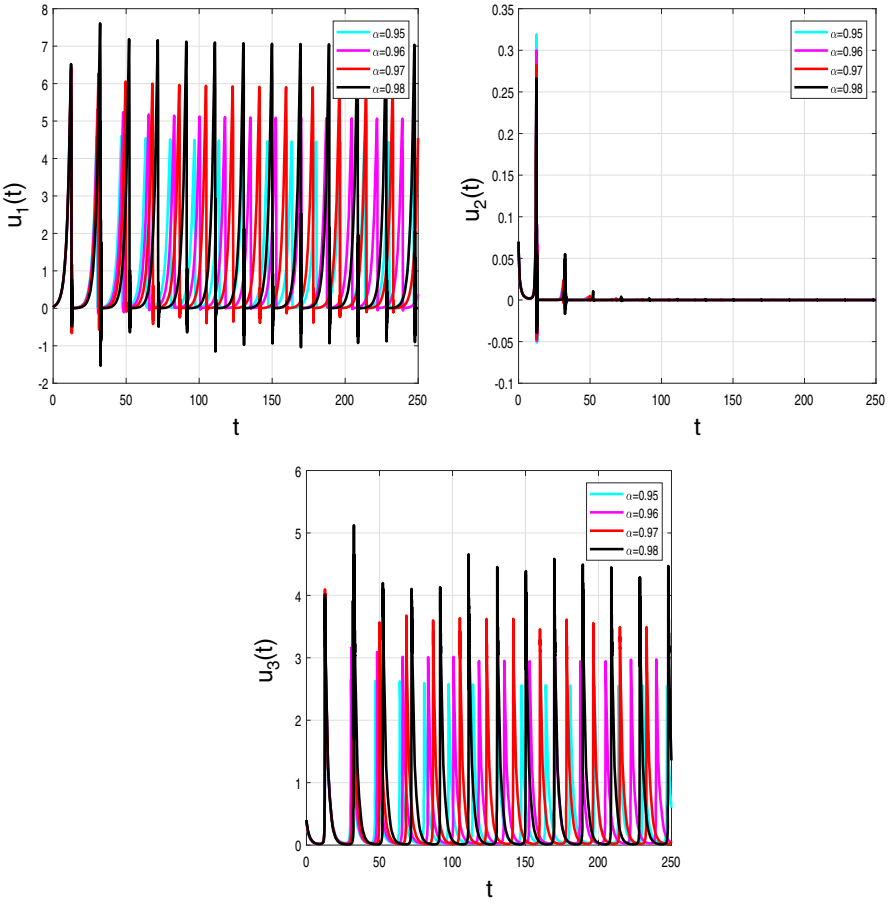

Fig. 16 Numerical simulations for $u_1(0) = 0.01, u_2(0) = 1.1$ and $u_3(0) = 0.05$ for $\xi_1 = 0.95, \xi_2 = 0.5, \xi_3 = 3.5, \xi_4 = 0.5, \xi_5 = 0.5, \xi_6 = 0.5$ and $\xi_7 = 1.5$

resembling phrases for components x_i, for $i = 1, 3$ to get $\|\mathcal{B}_i(u_i, t) - \mathcal{B}_i(u_i^*, t)\| \leq G_i\|u_i(t), u_i^*(t)\|$, for $i = 1, 3$. Hence, the Lipschitz condition works for $\mathcal{B}_2$, and contraction works for $0 \leq G_2 < 1$. Using the considered kernels (7) gives

$$\begin{aligned} u_1(t) &= u_1(0) + \frac{1-\sigma}{W(\sigma)}\mathcal{B}_1(u_1, t) + \frac{\sigma}{W(\sigma)\Gamma(\sigma)}\int_0^t (t-\zeta)^{\sigma-1}\mathcal{B}_1(\zeta, u_1)\mathrm{d}\zeta, \\ u_2(t) &= u_2(0) + \frac{1-\sigma}{W(\sigma)}\mathcal{B}_2(u_2, t) + \frac{\sigma}{W(\sigma)\Gamma(\sigma)}\int_0^t (t-\zeta)^{\sigma-1}\mathcal{B}_2(\zeta, u_2)\mathrm{d}\zeta, \\ u_3(t) &= u_3(0) + \frac{1-\sigma}{W(\sigma)}\mathcal{B}_3(u_3, t) + \frac{\sigma}{W(\sigma)\Gamma(\sigma)}\int_0^t (t-\zeta)^{\sigma-1}\mathcal{B}_3(\zeta, u_3)\mathrm{d}\zeta, \end{aligned} \tag{10}$$

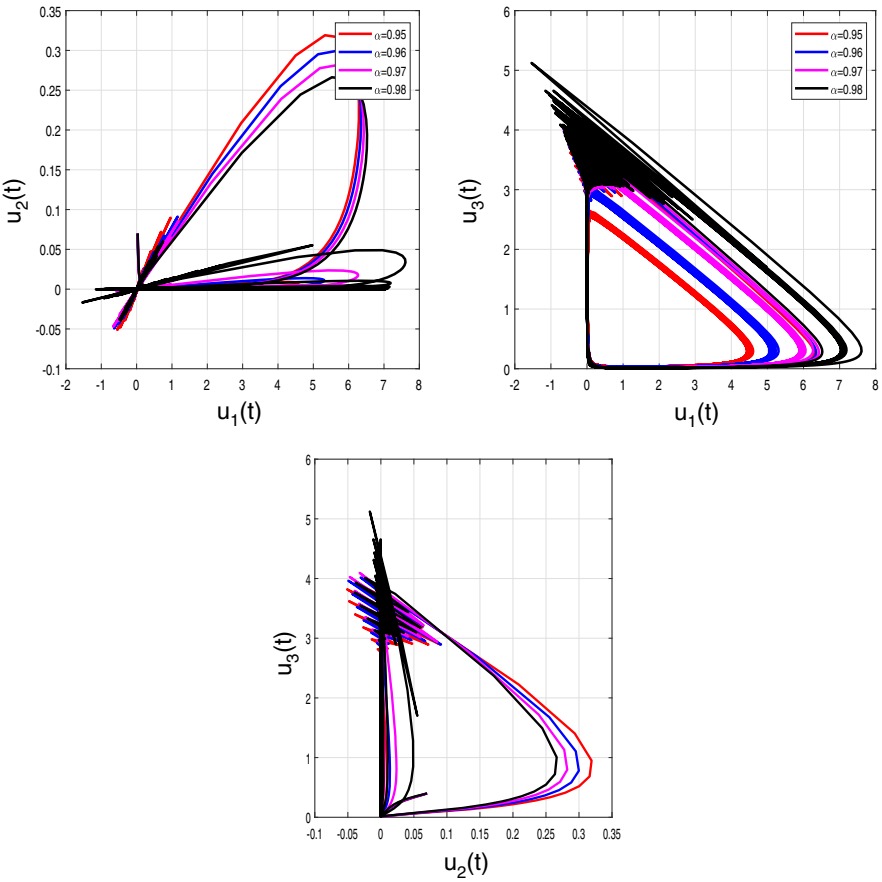

Fig. 17 Numerical simulations for $u_1(0) = 0.01, u_2(0) = 1.1$ and $u_3(0) = 0.05$ for $\xi_1 = 0.95, \xi_2 = 0.5, \xi_3 = 3.5, \xi_4 = 0.5, \xi_5 = 0.5, \xi_6 = 0.5$ and $\xi_7 = 1.5$

and

$$
\begin{aligned}
u_{1,n}(t) &= \frac{1-\sigma}{W(\sigma)}\mathcal{B}_1(u_{1,n-1},t) + \frac{\sigma}{W(\sigma)\Gamma(\sigma)}\int_0^t (t-\zeta)^{\sigma-1}\mathcal{B}_1(\zeta,u_{1,n-1})\mathrm{d}\zeta,\\
u_{2,n}(t) &= \frac{1-\sigma}{W(\sigma)}\mathcal{B}_2(u_{2.n-1},t) + \frac{\sigma}{W(\sigma)\Gamma(\sigma)}\int_0^t (t-\zeta)^{\sigma-1}\mathcal{B}_2(\zeta,u_{2,n-1})\mathrm{d}\zeta,\\
u_{3,n}(t) &= \frac{1-\sigma}{W(\sigma)}\mathcal{B}_3(u_{3,n-1},t) + \frac{\sigma}{W(\sigma)\Gamma(\sigma)}\int_0^t (t-\zeta)^{\sigma-1}\mathcal{B}_3(\zeta,u3,n-1)\mathrm{d}\zeta,
\end{aligned}
\tag{11}
$$

Then, we have

$$
\begin{aligned}
Z1_n(t) \equiv u_{1,n}(t) - u_{1,n-1}(t) &= \frac{1-\sigma}{W(\sigma)}\left[\mathcal{B}_1(u_{1,n-1},t) - \mathcal{B}_1(u_{1,n-2},t)\right]\\
&\quad + \frac{\sigma}{W(\sigma)\Gamma(\sigma)}\int_0^t (t-\zeta)^{\sigma-1}\left[\mathcal{B}_1(\zeta,u_{1,n-1}) - \mathcal{B}_1(\zeta,u_{1,n-2})\right]\mathrm{d}\zeta,\\
Z2_n(t) \equiv u_{2,n}(t) - u_{2,n-1}(t) &= \frac{1-\sigma}{W(\sigma)}\left[\mathcal{B}_2(u_{2,n-1},t) - \mathcal{B}_2(u_{2,n-2},t)\right]
\end{aligned}
$$

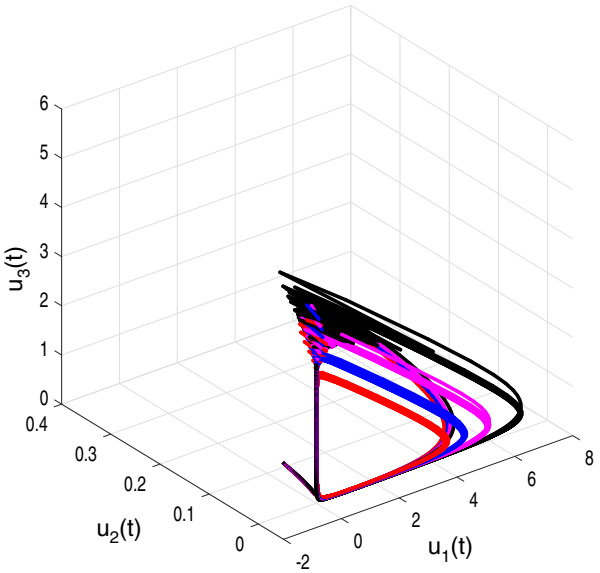

Fig. 18 Chaotic behaviour of solutions for $u_1(0) = 0.01, u_2(0) = 1.1$ and $u_3(0) = 0.05$ for $\xi_1 = 0.95, \xi_2 = 0.5, \xi_3 = 3.5, \xi_4 = 0.5, \xi_5 = 0.5, \xi_6 = 0.5$ and $\xi_7 = 1.5$

$$+\frac{\sigma}{W(\sigma)\Gamma(\sigma)}\int_0^t (t-\zeta)^{\sigma-1}\left[\mathcal{B}_2(\zeta, u_{2,n-1}) - \mathcal{B}_2(\zeta, u_{2,n-2})\right]\mathrm{d}\zeta,$$

$$Z3_n(t) \equiv u_{3,n}(t) - u_{3,n-1}(t) = \frac{1-\sigma}{W(\sigma)}\left[\mathcal{B}_3(u_{3,n-1}, t) - \mathcal{B}_3(u_{3,n-2}, t)\right]$$

$$+\frac{\sigma}{W(\sigma)\Gamma(\sigma)}\int_0^t (t-\zeta)^{\sigma-1}\left[\mathcal{B}_3(\zeta, u_{3,n-1}) - \mathcal{B}_3(\zeta, u_{3,n-2})\right]\mathrm{d}\zeta, \tag{12}$$

we state that

$$u_{i,n} = \sum_{j=1}^{n} Zi_j(t), i = 1, 2, 3.$$

Now, we take (12) and use the norm to have

$$\|Z1_n\| = \|u_{1,n}(t) - u_{1,n-1}(t)\| \leq \frac{1-\sigma}{W(\sigma)}\|\mathcal{B}_1(u_{1,n-1}, t) - \mathcal{B}_1(u_{1,n-2}, t)\| + \frac{p}{W(\sigma)\Gamma(\sigma)}$$

$$\times \| \int_0^t (t-\zeta)^{\sigma-1}\left[\mathcal{B}_1(u_{1,n-1}, t) - \mathcal{B}_1(u_{1,n-2}, t)\right]\mathrm{d}\zeta \|. \tag{13}$$

To satisfy the Lipschitz condition, we have

$$\|u_{1,n}(t) - u_{1,n-1}(t)\| \leq \frac{1-\sigma}{W(\sigma)}\chi_1\|u_{1,n-1} - u_{1,n-2}\|$$

$$+ \frac{p}{W(\sigma)\Gamma(\sigma)} \times \chi_1 \int_0^t (t-\zeta)^{\sigma-1}\|u_{1,n-1} - u_{1,n-2}\|\mathrm{d}\zeta, \tag{14}$$

and

$$\|Z1_n\| \leq \frac{1-\sigma}{W(\sigma)}\chi_1\|Z1_{n-1}\| + \frac{\sigma}{W(\sigma)\Gamma(\sigma)} \times \chi_1 \int_0^t (t-\zeta)^{\sigma-1}\|Z1_{n-1}(\zeta)\|\mathrm{d}\zeta, \tag{15}$$

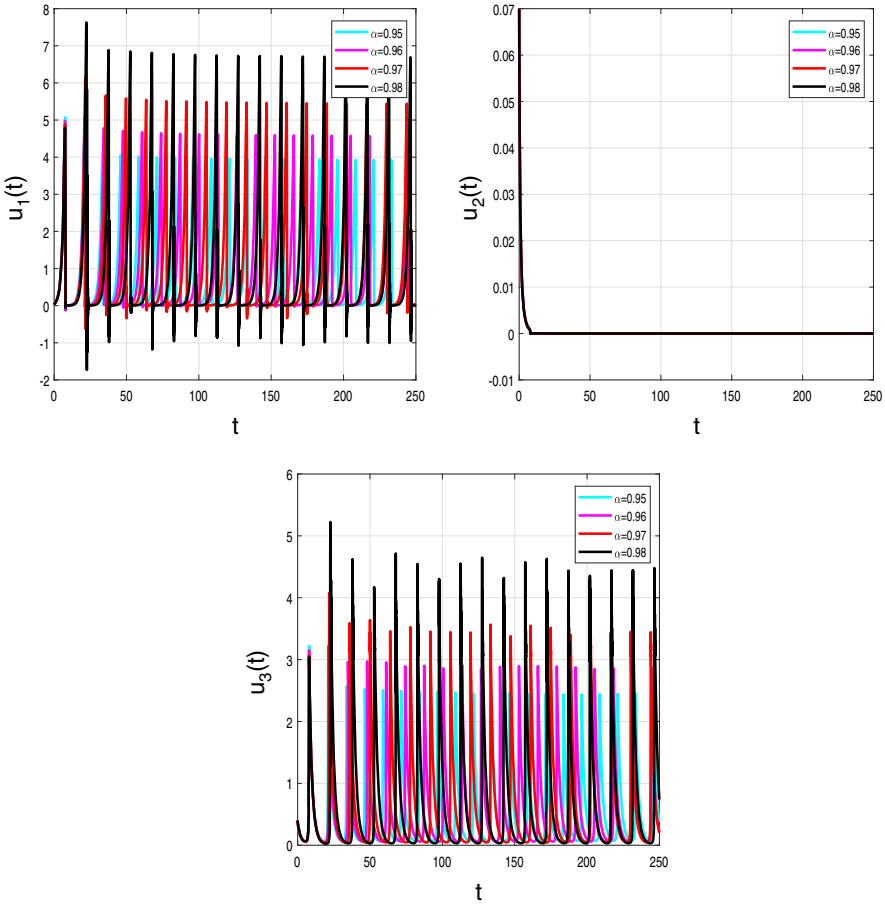

Fig. 19 Numerical simulations for $u_1(0) = 0.01$, $u_2(0) = 1.1$ and $u_3(0) = 0.05$ for $\xi_1 = 1.2$, $\xi_2 = 0.5$, $\xi_3 = 3.5$, $\xi_4 = 0.05$, $\xi_5 = 0.5$, $\xi_6 = 0.5$ and $\xi_7 = 1.5$

Equivalent expressions guard for rest elements:

$$\|Zi_n\| \leq \frac{1-\sigma}{W(\sigma)}\chi_1\|Zi_{n-1}\| + \frac{\sigma}{W(\sigma)\Gamma(\sigma)} \times \chi_1 \int_0^t (t-\zeta)^{\sigma-1}\|Zi_{n-1}(\zeta)\|\mathrm{d}\zeta, \quad i = 2, 3, \tag{16}$$

We take solutions $X_1(t)$, $X_2(t)$ and $X_3(t)$ exist for model (5) that indicates

$$\begin{aligned}\|u_1(t) - X_1(t)\| &\leq \frac{1-\sigma}{W(\sigma)}\left[\mathcal{B}_1(u_1,t) - \mathcal{B}_1(X_1,t)\right] \\ &\quad + \frac{\sigma}{W(\sigma)\Gamma(\sigma)}\int_0^t (t-\zeta)^{\sigma-1}\left[\mathcal{B}_1(u_1,t) - \mathcal{B}_1(X_1,t)\right]\mathrm{d}\zeta \\ &\leq \frac{1-\sigma}{W(\sigma)}\|\mathcal{B}_1(u_1,t) - \mathcal{B}_1(X_1,t)\| \\ &\quad + \frac{\sigma}{W(\sigma)\Gamma(\sigma)}\int_0^t (t-\zeta)^{\sigma-1}\|[\mathcal{B}_1(u_1,t) - \mathcal{B}_1(X_1,t)\|\mathrm{d}\zeta,\end{aligned} \tag{17}$$

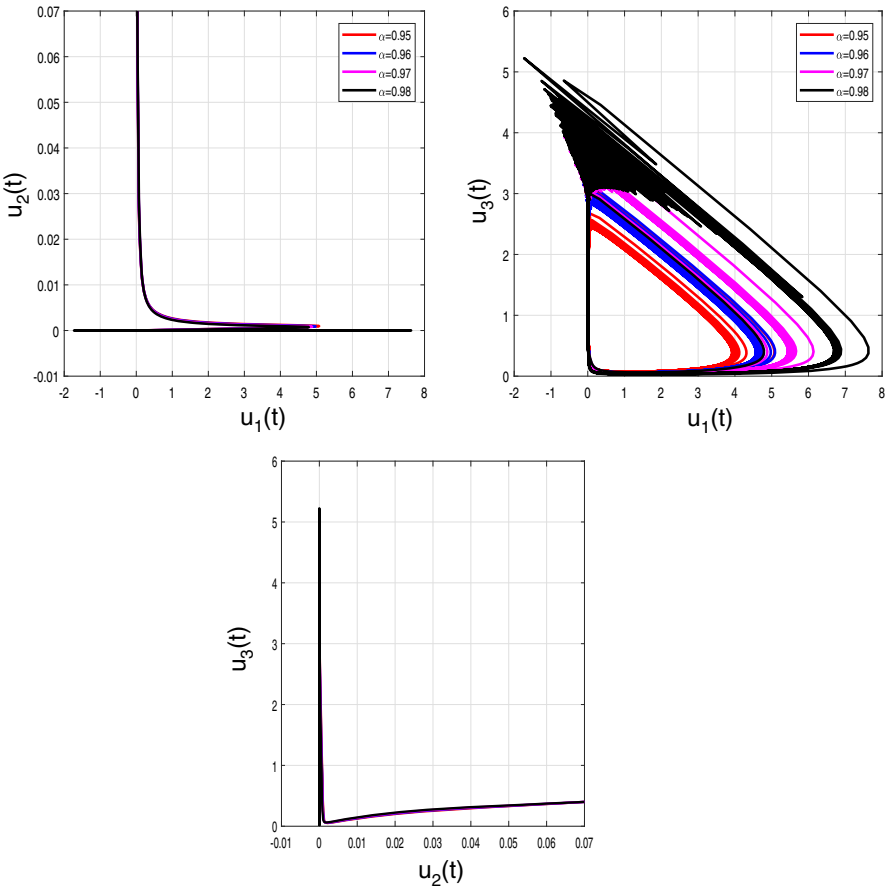

Fig. 20 Numerical simulations for $u_1(0) = 0.01$, $u_2(0) = 1.1$ and $u_3(0) = 0.05$ for $\xi_1 = 1.2$, $\xi_2 = 0.5$, $\xi_3 = 3.5$, $\xi_4 = 0.05$, $\xi_5 = 0.5$, $\xi_6 = 0.5$ and $\xi_7 = 1.5$

By regarding traits of the Lipschitz condition yields in

$$\|u_1(t) - X_1(t)\| \leq \frac{1-\sigma}{W(\sigma)}\chi_1\|u_1(t) - X_1(t)\| + \frac{\chi_1 t^\sigma}{W(\sigma)\Gamma(\sigma)}\|u_1(t) - X_1(t)\| \tag{18}$$

which results

$$\|u_1(t) - X_1(t)\|\left[1 - \frac{\chi_1(1-\sigma)}{W(\sigma)} + \frac{\chi_1 t^\sigma}{W(\sigma)\Gamma(\sigma)}\right] \leq 0 \tag{19}$$

with $\|u_1(t) - X_1(t)\| = 0$, it indicates $u_1(t) = X_1(t)$. Alike phrases exist for segments $u_i(t)$, $i = 2, 3$.Consequently, the fractional problem (5) owns a unique answer. □

Numerical Scheme

Now, we will apply the numerical technique to resolve the problem for simulations. The method has the following form:

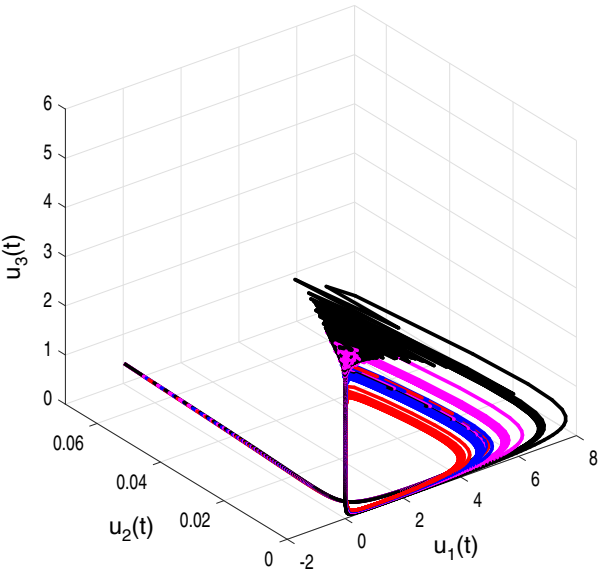

Fig. 21 Chaotic behaviour of solutions for $u_1(0) = 0.01, u_2(0) = 1.1$ and $u_3(0) = 0.05$ for $\xi_1 = 1.2, \xi_2 = 0.5, \xi_3 = 3.5, \xi_4 = 0.05, \xi_5 = 0.5, \xi_6 = 0.5$ and $\xi_7 = 1.5$

$$u_{n+1} = u_0 + \frac{1-\sigma}{W(\sigma)} f(u(t_n), t_n) + \frac{\sigma}{W(\sigma)} \sum_{q=0}^{n} \left\{ \frac{h^\sigma f(u_q, t_q)}{\Gamma(\sigma+2)} a_n - \frac{h^\sigma f(u_{q-1}, t_{q-1})}{\Gamma(\sigma+2)} b_n \right\} + E_n^\sigma, \tag{20}$$

where $a_n = (n+1-q)^\sigma (n-q+2+\sigma) - (n-q)^\sigma (n-q+2+2\sigma)$ and $b_n = (n+1-q)^{\sigma+1} - (n-1)^\sigma (n-q+1+\sigma)$ and the remaining term E_n^p is expressed by

$$E_n^\sigma = \frac{\sigma}{W(\sigma)\Gamma(\sigma)} \sum_{q=0}^{n} \int_{t_q}^{t_{q-1}} \frac{(\zeta - t_q)(\zeta - t_{q-1})}{2} \frac{\partial^2}{\partial \zeta^2} \times [f(u(\zeta), \zeta)]_{\zeta = \lambda_\zeta} (t_{n+1} - \zeta)^{\sigma-1} \mathrm{d}\zeta, \tag{21}$$

So, exercising the kernels, Eq. (10) changes to the following

$$\begin{aligned} u_1(t) &= u_1(0) + \frac{1-\sigma}{W(\sigma)} \mathcal{B}_1(u_1(t), t) + \frac{\sigma}{W(\sigma)\Gamma(\sigma)} \int_0^t (t-\zeta)^{\sigma-1} \mathcal{B}_1(\zeta, u_1(\zeta)) \mathrm{d}\zeta, \\ u_2(t) &= u_2(0) + \frac{1-\sigma}{W(\sigma)} \mathcal{B}_2(u_2(t), t) + \frac{\sigma}{W(\sigma)\Gamma(\sigma)} \int_0^t (t-\zeta)^{\sigma-1} \mathcal{B}_2(\zeta, u_2(\zeta)) \mathrm{d}\zeta, \\ u_3(t) &= u_3(0) + \frac{1-\sigma}{W(\sigma)} \mathcal{B}_3(u_3(t), t) + \frac{\sigma}{W(\sigma)\Gamma(\sigma)} \int_0^t (t-\zeta)^{\sigma-1} \mathcal{B}_3(\zeta, u_3(\zeta)) \mathrm{d}\zeta. \end{aligned} \tag{22}$$

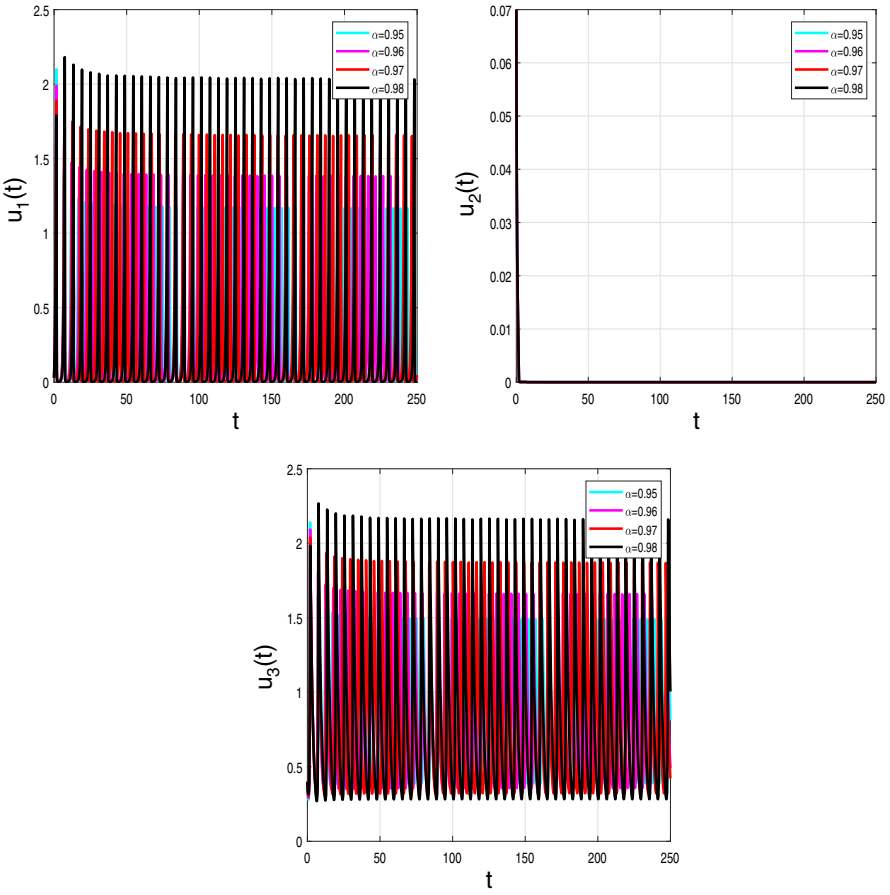

Fig. 22 Numerical simulations for $u_1(0) = 0.01, u_2(0) = 1.1$ and $u_3(0) = 0.05$ for $\xi_1 = 3.5, \xi_2 = 1.5, \xi_3 = 3.5, \xi_4 = 0.05, \xi_5 = 0.5, \xi_6 = 0.5$ and $\xi_7 = 1.5$

Thus, exercising the technique given in (20) at $t = t_{n+1}$, we own

$$\begin{aligned}
u_{1,n+1} &= u_{1,0} + \frac{1-\sigma}{W(\sigma)}\mathcal{B}_1(u_1(t_n), t_n) + \frac{\sigma}{W(\sigma)}\sum_{q=0}^{n}\left\{\frac{h^\sigma \mathcal{B}_1(u_{1,q}, t_q)}{\Gamma(\sigma+2)}a_n\right. \\
&\quad \left. - \frac{h^\sigma \mathcal{B}_1(u_{1,q-1}, t_{q-1})}{\Gamma(\sigma+2)}b_n\right\} + {}^1E_n^\sigma, \\
u_{2,n+1} &= u_{2,0} + \frac{1-\sigma}{W(\sigma)}\mathcal{B}_2(u_2(t_n), t_n) + \frac{\sigma}{W(\sigma)}\sum_{q=0}^{n}\left\{\frac{h^\sigma \mathcal{B}_2(u_{2,q}, t_q)}{\Gamma(\sigma+2)}a_n\right. \\
&\quad \left. - \frac{h^p \mathcal{B}_2(u_{2,s-1}, t_{s-1})}{\Gamma(p+2)}b_n\right\} + {}^2E_n^\sigma, \\
u_{3,n+1} &= u_{3,0} + \frac{1-\sigma}{W(\sigma)}\mathcal{B}_3(u_3(t_n), t_n) + \frac{\sigma}{W(\sigma)}\sum_{q=0}^{n}\left\{\frac{h^\sigma \mathcal{B}_3(u_{3,q}, t_q)}{\Gamma(\sigma+2)}a_n\right. \\
&\quad \left. - \frac{h^p \mathcal{B}_3(u_{3,q-1}, t_{q-1})}{\Gamma(\sigma+2)}b_n\right\} + {}^3E_n^\sigma,
\end{aligned} \tag{23}$$

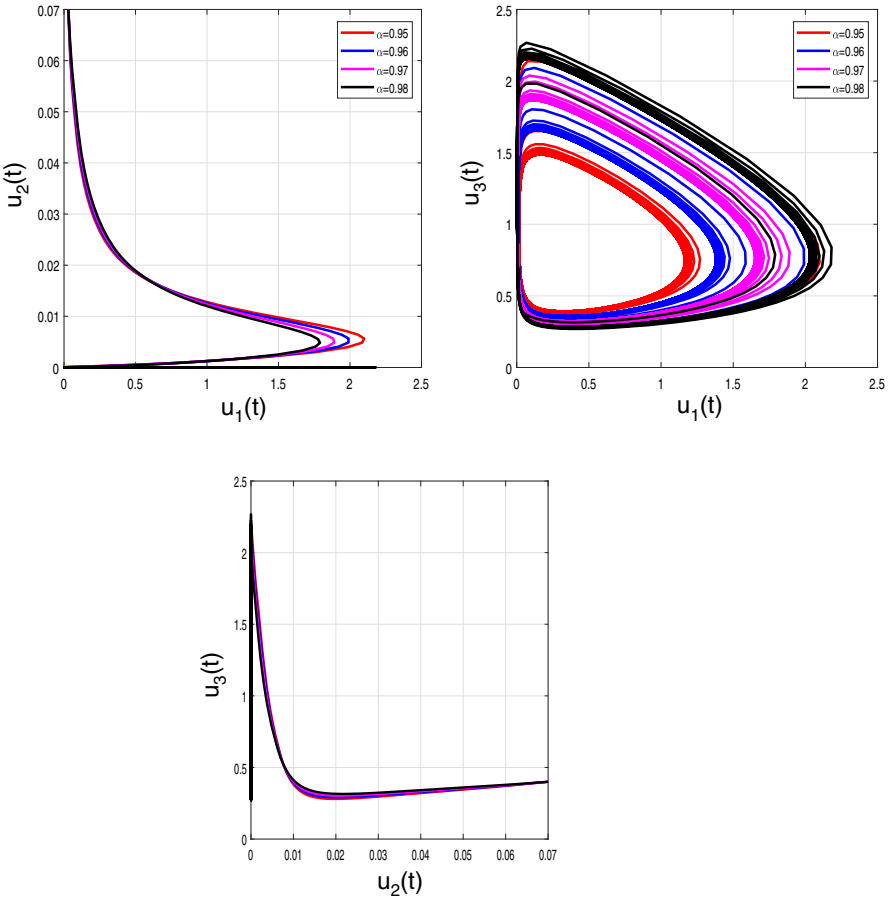

Fig. 23 Numerical simulations for $u_1(0) = 0.01$, $u_2(0) = 1.1$ and $u_3(0) = 0.05$ for $\xi_1 = 3.5$, $\xi_2 = 1.5$, $\xi_3 = 3.5$, $\xi_4 = 0.05$, $\xi_5 = 0.5$, $\xi_6 = 0.5$ and $\xi_7 = 1.5$

by $a_n = (n+1-q)^{\sigma}(n-q+2+\sigma) - (n-q)^{\sigma}(n-q+2+2\sigma)$, $b_n = (n+1-q)^{\sigma+1} - (n-q)^{p}(n-q+1+\sigma)$ and ${}^{i}E_n^{\sigma}$ for $i = 1, 2, 3$ is depicted as

$$ {}^{i}E_n^{\sigma} = \frac{\sigma}{W(\sigma)\Gamma(p)} \sum_{q=0}^{n} \int_{t_q}^{t_{q-1}} \frac{(\zeta - t_q)(\zeta - t_{q-1})}{2} \frac{\partial^2}{\partial \zeta^2} \left[\mathcal{B}_i(u(\zeta), \zeta)\right]_{\zeta=\lambda_\zeta} (t_{n+1} - \zeta)^{\sigma-1} \mathrm{d}\zeta, \tag{24} $$

Numerical Experiments

Now, we use the proposed numerical scheme [38] as discussed in the above-mentioned section to get the approximate solutions of the eco-epidemiological system as suggested in the present study under the novel fractional operator with the name of ABC. We solve the system for different values of fractional order σ. Figures 1, 2 and 3 show the results for different

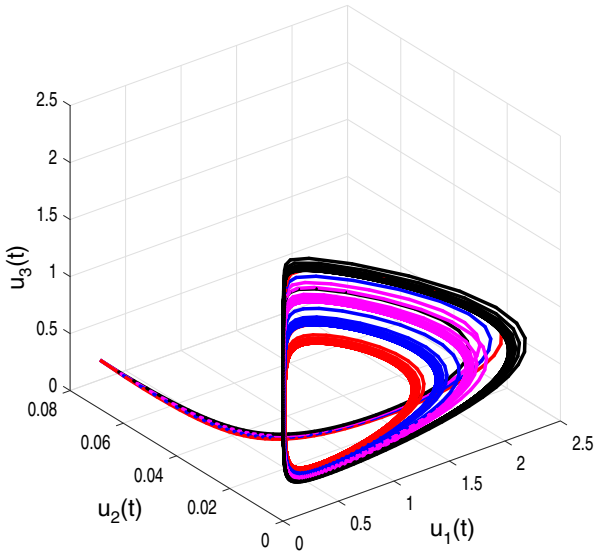

Fig. 24 Chaotic behaviour of solutions for $u_1(0) = 0.01, u_2(0) = 1.1$ and $u_3(0) = 0.05$ for $\xi_1 = 3.5, \xi_2 = 1.5, \xi_3 = 3.5, \xi_4 = 0.05, \xi_5 = 0.5, \xi_6 = 0.5$ and $\xi_7 = 1.5$

values of σ and also for different values of the ICs including $u_1(0) = 0.01, u_2(0) = 1.1$ and $u_3(0) = 0.05$ for $\xi_1 = 1.5, v_2 = 1.5, \xi_3 = 0.5, \xi_4 = 0.5, \xi_5 = 0.5, \xi_6 = 0.5$ and $\xi_7 = 0.5$. The fractional orders taken for these figures are 0.95, 0.96, 0.97 and 0.98. Indeed, the Figs. 4, 5 and 6 are dedicated to depict the results for σ values and with ICs given as $u_1(0) = 0.01, u_2(0) = 1.1$ and $u_3(0) = 0.05$ for $\xi_1 = 1.5, \xi_2 = 0.5, \xi_3 = 0.5, \xi_4 = 0.5, \xi_5 = 0.5, \xi_6 = 0.5$ and $\xi_7 = 0.5$; successfully. Similarly, Figs. 7, 8, 9, 10, 11, 12, 13, 14, 15, 16, 17, 18, 19, 20, 21, 22, 23, 24, 25, 26 and 27 are obtained to show the results for $\xi_1, \xi_2, \xi_3, \xi_4, \xi_5, \xi_6$ and ξ_7 along with the selected fractional orders for the parameter $\sigma > 0$.

In the Fig. 1, each state variable is simulated over considerably large time interval [0, 500] to understand dynamics of their behaviour. It is observed that the densities of susceptible prey, and predator populations highly fluctuate under selected ICs and the parameters whereas the density of the infected prey sharply decrease over a very small time interval and then goes to vanish as quickly as possible and this situation occurs because susceptible and the predator population are at greater variation.

If we closely look at the Fig. 2 then we realize that that patterns like limit cycles occur in the phase portrait forms under different values of σ and the parameters. Some strange chaotic type behavior is observed in the figure which is not possible to obtain with classical version of the eco-epidemiological system, that is, when $\sigma = 1$. Similarly, Fig. 3 shows 3-dimensional plot for the underlying system wherein, once again, chaotic type behavior with predator–prey limit cycles is observed. This phenomenon is highly obvious in natural situations as well. Thus, it is said that ABC operator is capable enough to capture the most natural occurrences in the world.

The Fig. 4 is obtained with a slight variation in the ξ_2 parameter that appears in the hunting cooperation functional as described in the Table 1. By decreasing ξ_2 from 1.5 to 0.5 in the Fig. 4, it is observed that the peaks of the fluctuations within the susceptible prey and predator populations decrease including the peak in the infected prey. However, there are still limit cycles having varying structures are observed as can be seen in the Figs. 5 (2D phase-plane diagrams) and 6 (3 dimensional dynamics). While keeping the ICs same and varying some values of the parameters, we observe drastic change in the dynamics of the

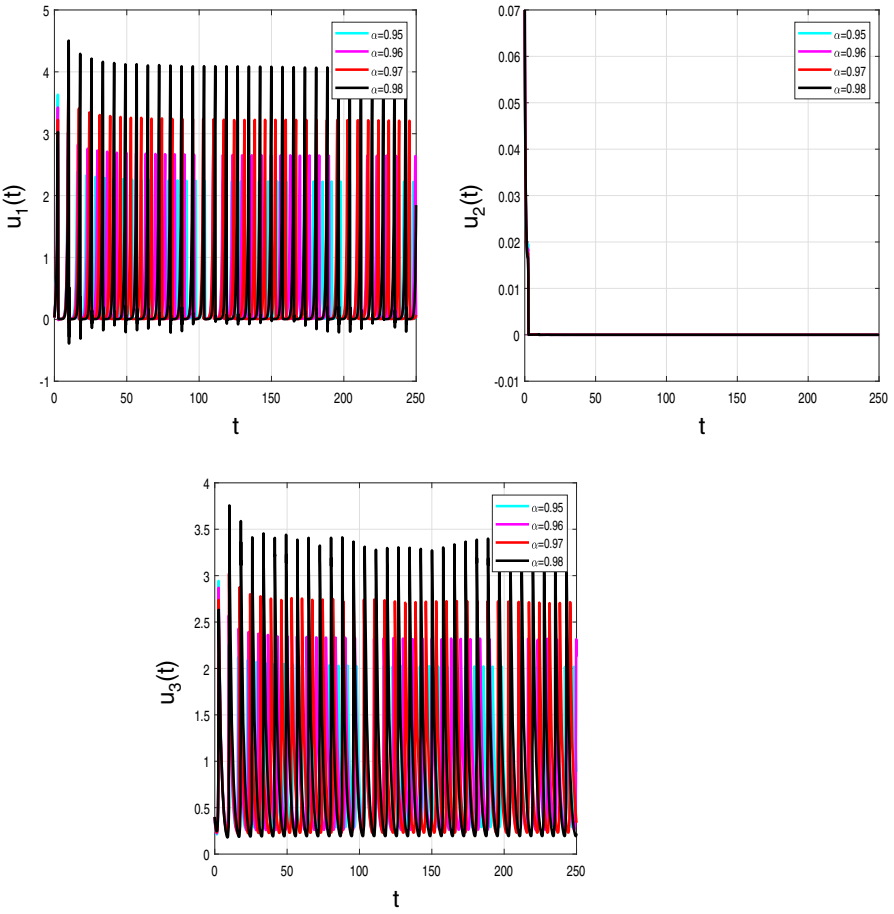

Fig. 25 Numerical simulations for $u_1(0) = 0.01$, $u_2(0) = 1.1$ and $u_3(0) = 0.05$ for $\xi_1 = 1.5$, $\xi_2 = 1.5$, $\xi_3 = 0.5$, $\xi_4 = 0.05$, $\xi_5 = 0.5$, $\xi_6 = 0.5$ and $\xi_7 = 0.5$

eco-epidemiological system as can be seen in the time series plots in the Fig. 7 wherein one can note that the not only peak of fluctuations decrease but the infected prey slightly increase also. One may also note that as value of fractional order σ approaches 1, the fluctuations increase. Some interesting limit cycles in the form of phase-planes and 3 dimensional plots are also depicted in the Figs. 8 and 9; respectively.

Looking at the Fig. 10, one can observe that there comes huge change in the behavior of all three populations when parameters are varied particularly the parameters ξ_3 and ξ_7 with little bit high values while ICs and the fractional order σ are still same as considered in previous figures. Limit cycles as shown in the Fig. 11 are reduced in size and this happens due to the fact that now there are not many fluctuations in the populations. Similarly, the Fig. 12 refers the chaotic behavior that lasts for smaller interval of time.

Likewise, upon carrying out numerous other simulations of the eco-epidemiological system as suggested in the present study under the novel fractional operator with the name of ABC, we have obtained interesting dynamics and patterns that were not not encountered with operators having no memory such as those classical ones also called integer-order deriva-

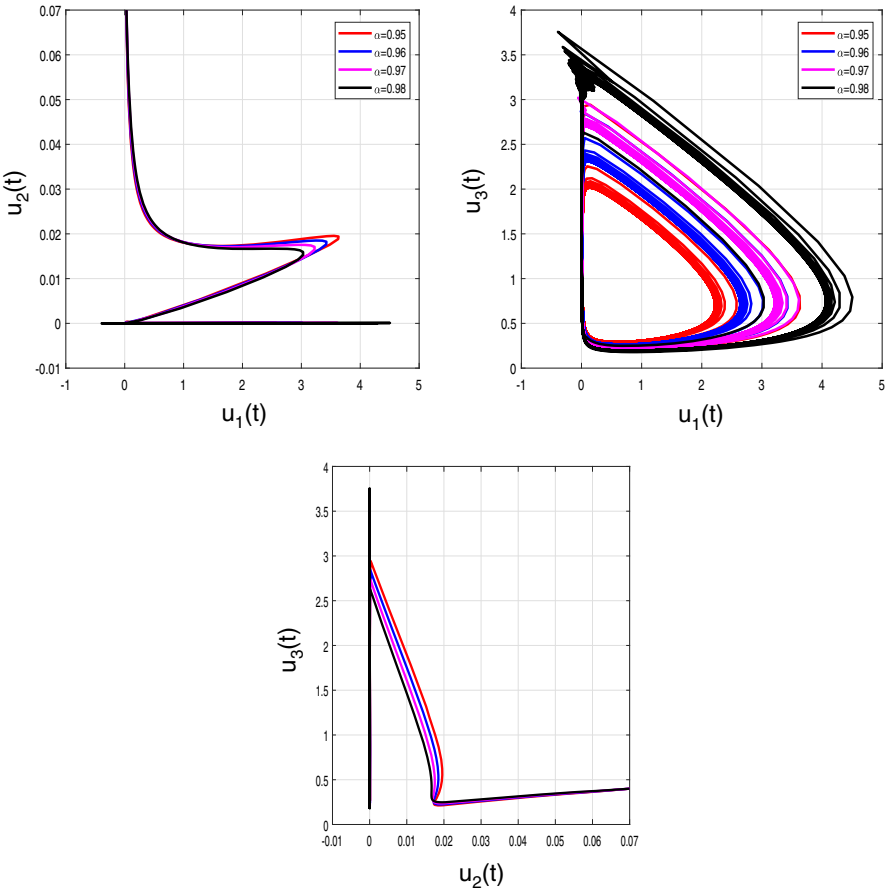

Fig. 26 Numerical simulations for $u_1(0) = 0.01$, $u_2(0) = 1.1$ and $u_3(0) = 0.05$ for $\xi_1 = 1.5$, $\xi_2 = 1.5$, $\xi_3 = 0.5$, $\xi_4 = 0.05$, $\xi_5 = 0.5$, $\xi_6 = 0.5$ and $\xi_7 = 0.5$

tives. These other simulations based upon time series, phase-portraits and 3 dimensional structures can be visualized in the Figs. 13, 14, 15, 16, 17, 18, 19, 20, 21, 22, 23, 24, 25, 26 and 27 wherein different parameters' values are taken into consideration in order to obtain the various kinds of behavior for the system via ABC operator.

Conclusion

In this research study, numerical simulations of the Prey–Predator system is investigated using the ABC operator. We used the theorem of fixed-point to establish the occurrence and uniqueness of the results of the underlying system. Employing numerical approach, solutions of the system are produced that depict quite interesting dynamical features not possible to achieve under the classical approach of differential calculus. To understand the influence of fractional order σ, numerical investigations are illustrated under engaging various fractional orders of σ. To explain the chaotic behavior in deep, we have tried various values of the

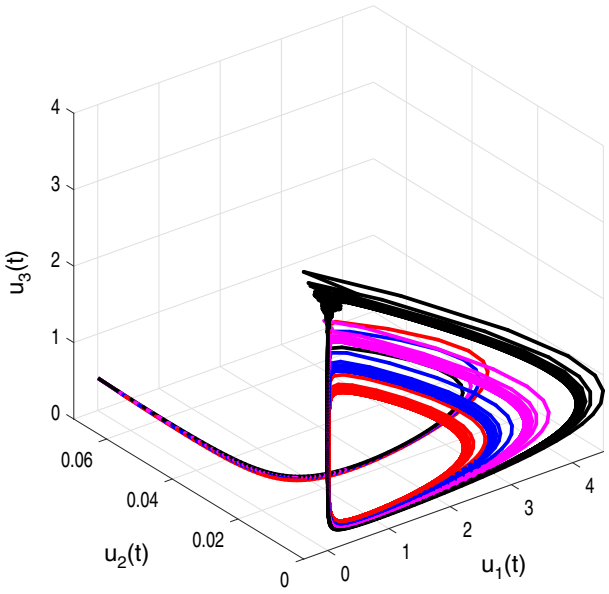

Fig. 27 Chaotic behaviour of solutions for $u_1(0) = 0.01, u_2(0) = 1.1$ and $u_3(0) = 0.05$ for $\xi_1 = 1.5, \xi_2 = 1.5, \xi_3 = 0.5, \xi_4 = 0.05, \xi_5 = 0.5, \xi_6 = 0.5$ and $\xi_7 = 0.5$

involved parameters in the model so that the state variables like susceptible prey, infected prey, and the predator populations could be visualized under ABC operator with different values of σ. It may be noted that such detailed analysis under the ABC operator has not been previously encountered in the existing literature for the eco-epidemiological system. Future studies would include the analysis of the discussed system with another operator called the Caputo-Fabrizio operator and some optimal control theory would also be discussed in the realm of fractional calculus.

Acknowledgements The authors would like to thank the reviewers for their valuable comments.

Author Contributions All authors have equal contribution.

Funding There is no funding.

Availability of data and materials No date used in this work.

Declarations

Ethics approval and consent to participate There is no ethics issue in this work.

Conflict of interest There is no conflict of interest.

References

1. Freedman, H.I.: Deterministic Mathematical Models in Population Ecology, vol. 57. Marcel Dekker, New York (1980)
2. Murray, J.D.: Mathematical Biology, 3rd edn. Springer, Berlin (2002)
3. Dubey, B., Upadhyay, R.K.: Persistence and extinction of one-prey and two-predator system. Nonlinear Anal. Model. Control **9**(4), 307–329 (2004)

4. Gakkhar, S., Singh, B., Naji, R.K.: Dynamical behavior of two predators competing over a single prey. BioSystems **90**(3), 808–817 (2007)
5. Kar, T.K., Batabyal, A.: Persistence and stability of a two prey one predator. Int. J. Eng. Sci. Technol. **2**(2), 174–190 (2010)
6. Samanta, G.P.: Analysis of a delay nonautonomous predator–prey system with disease in the prey. Nonlinear Anal. Model. Control **15**(1), 97–108 (2010). https://doi.org/10.15388/NA.2010.15.1.14367
7. Wang, W., Chen, L.: A predator–prey system with stage-structure for predator. Comput. Math. Appl. **33**(8), 83–91 (1997). https://doi.org/10.1016/j.mcm.2006.04.001
8. Bernard, O., Souissi, S.: Qualitative behavior of stages structure d populations: application to structural validation. J. Math. Biol. **37**(4), 291–308 (1998). https://doi.org/10.1007/s002850050130
9. Zhang, X., Chen, L., Neumann, A.U.: Th stage-structured predator–prey model and optimal harvesting policy. Math. Biosci. **168**(2), 201–210 (2000). https://doi.org/10.1016/S0025-5564(00)00033-X
10. Cui, J., Chen, L., Wang, W.: Th effect of dispersal on population growth with stage-structure. Comput. Math. Appl. **39**(1–2), 91–102 (2000). https://doi.org/10.1016/S0898-1221(99)00316-8
11. Cui, J., Takeuchi, Y.: A predator–prey system with a stage structure for the prey. Math. Comput. Model. **44**(11–12), 1126–1132 (2006). https://doi.org/10.1016/j.mcm.2006.04.001
12. Liu, S., Beretta, E.: A stage-structured predator–prey model of Beddington–DeAngelis type. SIAM J. Appl. Math. **66**(4), 1101–1129 (2006)
13. Chattopadhyay, J., Arino, O.: A predator–prey model with disease in the prey. Nonlinear Anal. **36**, 747–766 (1999)
14. Hadeler, K.P., Freedman, H.I.: Predator–prey populations with parasitic infection. J. Math. Biol. **27**, 609–631 (1989). https://doi.org/10.1007/bf00276947
15. Han, L., Ma, Z., Hethcote, H.W.: Four predator prey models with infectious diseases. Math. Comput. Model. **34**(7–8), 849–858 (2001). https://doi.org/10.1016/S0895-7177(01)00104-2
16. Zhou, X., Cui, J., Shi, X., et al.: A modified Leslie–Gower predator–prey model with prey infection. J. Appl. Math. Comput. **33**, 471–487 (2010). https://doi.org/10.1007/s12190-009-0298-6
17. Sweilam, N.H., Khader, M.M., Nagy, A.M.: Numerical solution of two- sided space-fractional wave equation using finite difference method. J. Comput. Appl. Math. **235**, 2832–2841 (2011). https://doi.org/10.1016/j.cam.2010.12.002
18. Duarte, J., Januario, C., Martins, N., Sardanyes, J.: Chaos and crises in a model for cooperative hunting a symbolic dynamics approach. Chaos **19**(4), 043102 (2009). https://doi.org/10.1063/1.3243924
19. Capone, F., Carfora, M.F., De Luca, R., Torcicollo, I.: Turing patterns in a reaction–diffusion system modeling hunting cooperation. Math. Comput. Simul. **165**, 172–180 (2019). https://doi.org/10.1016/j.matcom.2019.03.010
20. Cosner, C., DeAngelis, D., Ault, J., Olson, D.: Effects of spatial grouping on the functional response of predators. Theor. Popul. Biol. **56**(1), 65–75 (1999). https://doi.org/10.1006/tpbi.1999.1414
21. Pal, S., Pal, N., Samanta, S., Chattopadhyay, J.: Effect of hunting cooperation and fear in a predator–prey model. Ecol. Complex. **39**, 100770 (2019). https://doi.org/10.1016/j.ecocom.2019.100770
22. Ryu, K., Ko, W.: Asymptotic behavior of positive solutions to a predator–prey elliptic system with strong hunting cooperation in predators. Phys. A **531**, 121726 (2019). https://doi.org/10.1016/j.physa.2019.121726
23. Sen, D., Ghorai, S., Banerjee, S.M.: Allee effect in prey versus hunting cooperation on predator—enhancement of stable coexistence. Int. J. Bifurc. Chaos **29**(6), 1950081 (2019)
24. Singh, T., Dubey, R., Mishra, V.N.: Spatial dynamics of predator–prey system with hunting cooperation in predators and type I functional response. AIMS Math. **5**, 673–684 (2020). https://doi.org/10.3934/math.2020045
25. Song, D., Song, Y., Li, C.: Stability and turing patterns in a predator-prey model with hunting cooperation and Allee effect in prey population. Int. J. Bifurc. Chaos **30**(09), 2050137 (2020). https://doi.org/10.1142/S0218127420501370
26. Wu, D., Zhao, M.: Qualitative analysis for a diffusive predator–prey model with hunting cooperative. Phys. A **515**, 299–309 (2019). https://doi.org/10.1016/j.physa.2018.09.176
27. Yan, S., Jia, D., Zhang, T., Yuan, S.: Pattern dynamics in a diffusive predator–prey model with hunting cooperations. Chaos Solitons Fractals **130**, 109428 (2020). https://doi.org/10.1016/j.chaos.2019.109428
28. Yavuz, M., Sene, N.: Stability analysis and numerical computation of the fractional predator–prey model with the harvesting rate. Fractal Fract. **4**(3), 35 (2020). https://doi.org/10.3390/fractalfract4030035
29. Hashemi, M.S., PartoHaghighi, M., Bayram, M.: On numerical solution of the time-fractional diffusion-wave equation with the fictitious time integration method. Eur. Phys. J. Plus **134**(10), 488 (2019). https://doi.org/10.1140/epjp/i2019-12845-1

30. Inc, M., Parto-Haghighi, M., Akinlar, M.A., Chu, Y.M.: New numerical solutions of fractional-order Korteweg-de Vries equation. Results Phys. **19**, 103326 (2019). https://doi.org/10.1016/j.rinp.2020.103326
31. Inc, M., Partohaghighi, M., Akinlar, M.A., Agarwal, P., Chu, Y.M.: New solutions of fractional-order Burger–Huxley equation. Results Phys. **18**, 103290 (2019). https://doi.org/10.1016/j.rinp.2020.103290
32. Partohaghighi, M., Ink, M., Baleanu, D., Moshoko, S.P.: Ficitious time integration method for solving the time fractional gas dynamics equation. Therm. Sci. **23**(Suppl. 6), 2009–2016 (2019). https://doi.org/10.2298/TSCI190421365P
33. Ahmad, Zubair, Ali, Farhad, Khan, Naveed, Khan, Ilyas: Dynamics of the fractal-fractional model of a new chaotic system of integrated circuit with Mittag–Leffler kernel. Chaos Solitons Fractals **153**, 111602 (2021). https://doi.org/10.1016/j.chaos.2021.111602
34. Murtaza, S., Kumam, P., Ahmad, Z., Sitthithakerngkiet, K., Ali, I.E.: Finite Difference simulation of fractal-fractional model of electro-osmotic flow of Casson fluid in a micro channel. IEEE Access **10**, 26681–26692 (2022). https://doi.org/10.1109/ACCESS.2022.3148970
35. Ahmad, Zubair, Bonanomi, Giuliano, di Serafino, Daniela, Giannino, Francesco: Transmission dynamics and sensitivity analysis of pine wilt disease with asymptomatic carriers via fractal-fractional differential operator of Mittag–Leffler kernel. Appl. Numer. Math. **185**, 446–465 (2023). https://doi.org/10.1016/j.apnum.2022.12.004
36. Ahmad, Zubair, Arif, Muhammad, Ali, Farhad, Khan, Ilyas, SooppyNisar, Kottakkaran: A report on COVID-19 epidemic in Pakistan using SEIR fractional model. Sci. Rep. **17;10**(1), 22268 (2020). https://doi.org/10.1038/s41598-020-79405-9
37. Ahmad, Z., El-Kafrawy, S.A., Alandijany, T.A., Giannino, F., Mirza, A.A., El-Daly, M.M., Faizo, A.A., Bajrai, L.H., Kamal, M.A.: A global report on the dynamics of COVID-19 with quarantine and hospitalization: a fractional order model with non-local kernel. Comput. Biol. Chem. **98**, 107645 (2022). https://doi.org/10.1016/j.compbiolchem.2022.107645
38. Toufik, M., Atangana, A.: New numerical approximation of fractional derivative with non-local and non-singular kernel: application to chaotic models. Eur. Phys. J. Plus **132**, 444 (2017)